AC OPF for Smart Distribution Networks: An Efficient and Robust Quadratic Approach

John F. Franco, *Member, IEEE*, Luis F. Ochoa, *Senior Member, IEEE*, and Rubén Romero, *Senior Member, IEEE*

Abstract—Smart grid schemes in which multiple network elements and participants are managed for the benefit of the distribution network (e.g., energy loss reduction, restoration, etc.) require sophisticated algorithms to control them in the most suitable manner while catering for network constraints. Such a complex decision making process can be solved by tailoring the ac optimal power flow (OPF) problem to the corresponding smart grid scheme. Non-linear programming ac OPF formulations, however, can suffer from scalability and robustness issues which in turn might limit their adoption. Here, a novel quadratic programming formulation is proposed and compared against the non-linear, quadratically constrained, and linearized approaches. Two cases are carried out to assess their performance: 1) management of distributed generation units to maximize renewable energy harvesting (continuous control variables) and 2) control of capacitors to minimize energy losses (discrete control variables). The results demonstrate that the proposed quadratic approach significantly outperforms the more conventional formulations in both computational efficiency and robustness. This makes it a suitable alternative to be at the heart of the decision making of complex, real-time schemes to be adopted by future smart distribution networks.

Index Terms—Distribution networks, non-linear programming, optimal power flow, quadratically constrained programming, quadratic programming, smart grids.

I. INTRODUCTION

THE INCREASING need for more reliable power supply, higher energy efficiency, the connection of small-to-medium scale renewable generation, and the electrification of transport pose significant challenges to the operation of distribution networks originally designed to only cope with a well understood demand. This new scenario where customers can consume and/or generate electricity requires the intelligent operation of all network elements and participants in order to effectively manage technical issues and, thus, avoid or defer otherwise required network reinforcements. These future

J. F. Franco is with the Universidade Estadual Paulista UNESP, Rosana 19274-000, Brazil (e-mail: j.f.franco@ieee.org).

L. F. Ochoa is with the Department of Electrical and Electronic Engineering, University of Melbourne, Parkville, VIC 3010, Australia, and also with the School of Electrical and Electronic Engineering, University of Manchester, Manchester M13 9PL, U.K. (e-mail: luis_ochoa@ieee.org).

R. Romero is with the Faculdade de Engenharia de Ilha Solteira, Universidade Estadual Paulista UNESP, Ilha Solteira 15385-000, Brazil (e-mail: ruben@dee.feis.unesp.br).

Smart Distribution Networks, however, will require sophisticated, scalable, and robust control algorithms designed to deal with the different challenges faced by utilities (e.g., energy loss reduction, voltage control, restoration, etc.) [1].

Although rule-based, coordinated control is traditionally adopted by utilities (e.g., localized control of on-load tap changing transformers), the increased complexity brought by a large number of network elements and participants can reduce its effectiveness. In this context, optimization approaches can potentially unlock the benefits from the holistic, centralized management of the distribution network. One of these approaches is the well-known AC Optimal Power Flow (OPF), which can be tailored for smart distribution networks [2]–[4].

The solution of a conventional power flow problem makes it possible to know the steady-state operation of a distribution network, i.e., voltages, power flows, and other variables of interest can be calculated. However, if some variables are controllable, such as the injection of generation units or the tap position of transformers, the operation of the network can be optimized according to the objectives of the utility (e.g., energy loss minimization, renewable generation harvesting maximization, etc.). The best set of control actions are determined by solving the AC OPF problem [5], [6].

In the context of smart distribution networks, different AC OPF-based methods have been proposed to achieve different objectives from both the planning [7]–[9] and control [2], [10]–[20] perspectives. For the former, this includes the maximization of renewable distributed generation (DG) capacity considering thermal and voltage limits [7], [8], as well as fault levels [9], and the minimization of power or energy losses by optimally allocating DG plants [10], [11]. More recently, the optimal (real-time or short-term) operation of smart distribution networks have been investigated considering the control of network elements (e.g., voltage regulation devices, capacitors, switches) and participants (e.g., DG plants) to cater for different objectives. The minimization of DG curtailment to deal with thermal and voltage constraints, in some cases in combination with the control of network elements, has been the main objective in [2], [12], and [13]. The minimization of losses have also been studied considering volt-var control [14]–[16] and reconfiguration [17]–[20]. The post-fault restoration problem, which looks for the best configuration that minimizes the affected customers, was investigated in [21].

AC OPF formulations adopted in the literature range from non-linear to linear. Most of the above studies

considered non-linear formulations [3], [7]–[15], [17] which can be developed in a straightforward manner. Nonetheless, in an attempt to improve scalability and computational time, alternative convex formulations have also been explored. This includes linear programming [16], [22], quadratically constrained [2], [18], [19], and semi-definite programming [4].

Since the seminal work of Carpenter [5], different OPF formulations have been investigated to increase their ability to cater for larger and more complex problems [23]. Such improvements are crucial for the optimal operation of future smart distribution networks due to their size and the number of controllable elements but also due to the presence of discrete variables (e.g., tap changers, status of switches, etc.). In this context, novel convex formulations allow to significantly improve scalability and guarantee finding the optimal solution of the problem (unlike conventional non-linear and non-convex formulations). In recent years, convex (although non-linear) formulations have been proposed for the AC OPF problem including relaxed conic [24], [25], convex semi-definite [26], [27], and quadratically constrained [2], [18], [19], [28] programming models.

Although quadratic programming (QP) formulations have been investigated for the AC OPF in transmission networks [29]–[31], these approaches require a sequential solution, which increases the complexity of the formulation. In [32], a QP formulation was proposed for distribution networks. However, non-linear terms related to power losses were neglected, thus resulting in errors in the voltage calculation.

A QP formulation for the AC OPF in smart distribution networks is proposed in this work. This novel approach uses linear constraints to represent power losses and, hence, results in a compromise between accuracy, performance, and robustness. In order to demonstrate and quantify the benefits of this novel model, formulations for the AC OPF problem are compared: non-linear programing (NLP), quadratically constrained programming (QCP), linearized models, and the novel QP formulation. Two cases are carried out to assess quality of the solution and computational time: (1) management of DG units to maximize renewable energy harvesting (continuous control variables); and, (2) control of capacitors to minimize energy losses (discrete control variables). Four tests were considered to assess scalability.

II. FORMULATIONS FOR THE AC OPTIMAL POWER FLOW

The AC OPF problem can be defined as a mathematical problem in which an objective function is minimized over a set of control variables (X), subject to a set of constraints (1).

$$\min \ f(X)$$
$$\text{subject to: } h(X) = 0; \ g(X) \leq 0 \tag{1}$$

The objective function $f(X)$ can be the minimization of energy losses, DG curtailment, etc., while the constraints are typically the active and reactive power balances (constraints $h(X)$), the voltage and thermal limits as well as the limits of the control variables (constraints $g(X)$).

In this section, non-linear, quadratically constrained and quadratic formulations are presented adopting similar structures and variables to emphasize their differences. To illustrate this, the same objective function is considered: the minimization of energy losses by dispatching DG units.

For simplicity, the distribution network is assumed to have a balanced operation (an extension for unbalanced networks is presented in the Appendix). In addition, the latter two formulations exploit the fact that most networks operate radially and, therefore, it is not necessary to consider explicitly the phase angle. Meshed networks, however, can also be catered for by incorporating additional constraints that represent the second Kirchhoff's law in terms of the voltage phase angle.

A. Non-Linear Programming Formulation

The AC OPF can be modeled as a non-linear optimization model defined by (2)-(11) in which the state variables are the voltage magnitude ($V_{n,t}$) and the voltage phase angle ($\theta_{n,t}$) [6]. In that model, L, N, DG, and T are the sets of lines, nodes, DG units, and time periods, respectively. G_{mn} and B_{mn} are the real and imaginary parts of the impedance of line mn. $I^{sqr}_{mn,t}$, $P_{mn,t}$, and $Q_{mn,t}$ are the square of the current magnitude, and the active and reactive powers through line mn (leaving node m) in time period t. R_{mn} and $\bar{I}^2_{mn}$ are the resistance and the current limit of line mn. $P^g_{m,t}$ and $Q^g_{m,t}$ are the active and reactive powers generated at node m, while $P^d_{m,t}$ and $Q^d_{m,t}$ are the active and reactive powers demanded also at node m. The upper and lower voltage limits are represented by $\overline{V}$ and $\underline{V}$. $\overline{P}^g_m$, $\overline{Q}^g_m$ and $\overline{pf}_m$, are the limits for the generation and the power factor of the DG unit at node m. The duration of the time period t is given by Δ_t.

The objective function minimizes energy losses in the lines over a time horizon (2), and the control variables are the power injections of the DG units, i.e., it is assumed they are dispatchable. The operational constraints are the limits for the voltage magnitude, the current capacity of the lines, and the power limits of the DG units. In this particular formulation, the active and reactive power balances in a node are given by (3) and (4), respectively; the power flows through the lines are defined by (5) and (6). The square of the current through line mn is defined by (7) and its limit is represented by (8). Constraints (9) and (10) correspond to the limits of the DG units (additional constraints such as thermal limits can also be incorporated). Shunt susceptance of the lines are not considered in this formulation but can also be incorporated.

$$\min \sum_{t \in T} \sum_{mn \in L} \Delta_t R_{mn} I^{sqr}_{mn,t} \tag{2}$$

subject to:

$$\sum_{n \in N} P_{mn,t} = P^g_{m,t} - P^d_{m,t} \qquad \forall t \in T, m \in N \tag{3}$$

$$\sum_{n \in N} Q_{mn,t} = Q^g_{m,t} - Q^d_{m,t} \qquad \forall t \in T, m \in N \tag{4}$$

$$P_{mn,t} = V^2_{n,t} G_{mn} - V_{m,t} V_{n,t} \left(G_{mn} \cos \theta_{mn,t} + B_{mn} \sin \theta_{mn,t} \right)$$
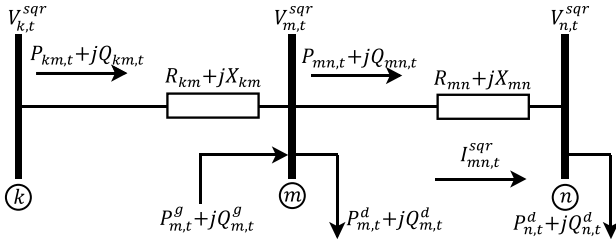$$\forall t \in T, m \wedge n \in N \tag{5}$$

Fig. 1. Illustrative example of the state variables for the QCP formulation.

$$Q_{mn,t} = -V_{n,t}^2 B_{mn} + V_{m,t}V_{n,t}\big(G_{mn}\sin\theta_{mn,t} - B_{mn}\cos\theta_{mn,t}\big)$$
$$\forall t \in T, m \wedge n \in N \qquad (6)$$

$$I_{mn,t}^{sqr} = \big(P_{mn,t}{}^2 + Q_{mn,t}{}^2\big)/V_{m,t}^2 \qquad \forall t \in T, mn \in L$$
$$\qquad (7)$$

$$I_{mn,t}^{sqr} \le \overline{I}_{mn}^2 \qquad \forall t \in T, mn \in L \qquad (8)$$

$$0 \le P_{m,t}^g \le \overline{P}_m^g \qquad \forall t \in T, m \in DG \qquad (9)$$

$$\big|Q_{m,t}^g\big| \le \min\Big(\overline{Q}_m^g, P_{m,t}^g \tan\Big(\arccos\big(\overline{pf}_m^g\big)\Big)\Big),$$
$$\forall t \in T, m \in DG \qquad (10)$$

$$\underline{V} \le V_{m,t} \le \overline{V} \qquad \forall t \in T, m \in N \qquad (11)$$

The above formulation is a NLP model due to the product of variables and non-linear functions (sine and cosine). Although some of the constraints can be defined in different ways, the adopted formulation helps understanding the transition towards the convex approaches later presented.

B. Quadratically Constrained Programming Formulation

The QCP formulation for the AC OPF in distribution networks is defined by (12)-(18) as a relaxed representation of the AC OPF (as proposed in [33]). Considering that distribution networks are usually operated radially, the mathematical model uses the square of the voltage magnitude ($V_{m,t}^{sqr}$), as well as the power and the current flows through the lines as the state variables, i.e., the voltage angle is not considered explicitly in the formulation [34].

In this QCP model, the operation of the network is represented through the variables $V_{n,t}^{sqr}$, $I_{mn,t}^{sqr}$, $P_{mn,t}$, and $Q_{mn,t}$ for line *mn*, as illustrated in Fig. 1. $P_{mn,t}$ is the active power flow leaving node *m* through line *mn*, while the active power arriving node *n* is $P_{mn,t} - R_{mn}I_{mn,t}^{sqr}$. X_{mn} and Z_{mn} are the reactance and impedance of line *mn*.

The objective function (12), the minimization of the energy losses, remains as in (2). Equations (14) and (15) are the balance of active and reactive powers in node *m*, respectively. The voltage drop in a line is calculated in terms of the power flow through the line and its electrical parameters, as defined by (16); this equation is obtained after eliminating the voltage angle as proposed in [34]. Moreover, the voltage limits are enforced by (17).

$$\min \sum_{t \in T} \sum_{mn \in L} \Delta_t R_{mn} I_{mn,t}^{sqr} \qquad (12)$$
$$\text{subject to: } (8)-(10) \qquad (13)$$

$$\sum_{km \in L}\big(P_{km,t} - R_{km}I_{km,t}^{sqr}\big) - \sum_{mn \in L} P_{mn,t} = P_{m,t}^g - P_{m,t}^d$$
$$\forall t \in T, m \in N \qquad (14)$$

$$\sum_{km \in L}\big(Q_{km,t} - X_{km}I_{km,t}^{sqr}\big) - \sum_{mn \in L} Q_{mn,t} = Q_{m,t}^g - Q_{m,t}^d$$
$$\forall t \in T, m \in N \qquad (15)$$

$$V_{m,t}^{sqr} - V_{n,t}^{sqr} = 2\big(R_{mn}P_{mn,t} + X_{mn}Q_{mn,t}\big) - Z_{mn}^2 I_{mn,t}^{sqr}$$
$$\forall t \in T, mn \in L \qquad (16)$$

$$\underline{V}^2 \le V_{m,t}^{sqr} \le \overline{V}^2 \qquad \forall t \in T, m \in N \qquad (17)$$

$$V_{m,t}^{sqr} I_{mn,t}^{sqr} \ge P_{mn,t}^2 + Q_{mn,t}^2 \qquad \forall t \in T, mn \in L \qquad (18)$$

Constraint (18) is a quadratic constraint which is a relaxed version of the relation between apparent power, current and voltage in a line. Originally, this relation is a non-linear equation in which the apparent power is equal to the product of the voltage and the current. Since (12)-(17) are linear constraints, the mathematical formulation (12)-(18) is a QCP convex model (although non-linear) for the AC OPF. However, as this is a relaxed model, to ensure the validity of the solution it is necessary to carry out a check to ensure the equality in (18). As demonstrated in [35], for the QCP relaxation to be exact it is sufficient to have a convex objective function that is strictly increasing with $I_{mn,t}^{sqr}$ (true for (12), losses) and no lower bounds on power injections.

C. Quadratic Programming Formulation

The proposed QP model is an approximation for the AC OPF which builds on the previously defined QCP. This novel QP formulation is shown in (19)–(33). The objective function (19), the minimization the energy losses, now considers the sum of quadratic terms related to the power through the lines in which estimated values for the voltage are used ($\tilde{V}_{m,t}^{sqr}$). The accent "$\sim$" indicates the term is the estimated value of the corresponding variable. Constraints (21)-(33) can be classified into four blocks: a) limits of DG units and bus voltages, represented by (20); b) active and reactive power balances, (21) and (22); c) second Kirchhoff's law, i.e., line voltage drops, (23); and d) line current limits, (24)-(33).

The left-hand side of (24) imposes a limit for the apparent power flow through the lines; the square of the voltage (variable) and the upper current limit (constant) are used to transform the quadratic constraint (18) into a linear expression. The terms on the right-hand side of (24) are the linear approximations of $P_{mn,t}^2$ and $Q_{mn,t}^2$. This piecewise linearization estimates the square value of a variable using auxiliary ones that are, in turn, related to a given number of discretization intervals (Λ). For instance, $\Delta_{mn,t,\lambda}^{P}$ variables are used to approximate $P_{mn,t}^2$. The absolute value of the approximated variable is calculated as the sum of two non-negative variables ($P_{mn,t}^+$ and $P_{mn,t}^-$) according to (25) and (27). Finally, the square of the approximated variable is calculated as the weighted sum of the auxiliary ones, as shown in the right-hand side of (24). Here, the weight $\rho_{mn,\lambda}$ is the slope of the line segment that approximates the square function in the λ-th discretization interval, while $\overline{\Delta}_{mn}$ is the upper limit of the auxiliary variables in the piecewise linearization. Conditions related to
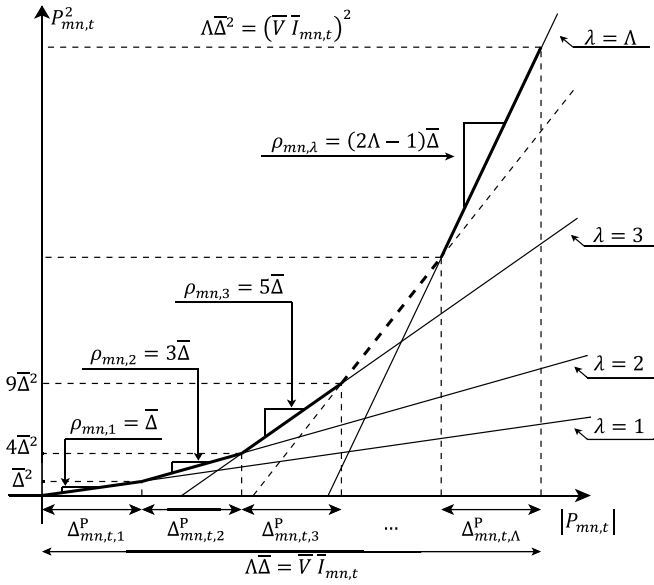
Fig. 2. Piecewise linearization of $P^2_{mn,t}$.

the non-negativity of the variables, their limits, and the definition of the parameters used in this approximation are given by (29)-(33). This approach is illustrated in Fig. 2.

$$\min \sum_{t \in T} \sum_{mn \in L} \Delta_t R_{mn} \frac{P^2_{mn,t} + Q^2_{mn,t}}{\tilde{V}^2_{m,t}} \tag{19}$$

subject to: (9), (10), (17) $\tag{20}$

$$\sum_{km \in L} \left[P_{km,t} + \frac{R_{km}}{\tilde{V}^2_{k,t}} \left(\tilde{P}_{km,t} P_{km,t} + \tilde{Q}_{km,t} Q_{km,t} \right) \right]$$
$$- \sum_{mn \in L} P_{mn,t} = P^g_{m,t} - P^d_{m,t} \quad \forall t \in T, m \in N \tag{21}$$

$$\sum_{km \in L} \left[Q_{km,t} + \frac{X_{km}}{\tilde{V}^2_{k,t}} \left(\tilde{P}_{km,t} P_{km,t} + \tilde{Q}_{km,t} Q_{km,t} \right) \right]$$
$$- \sum_{mn \in L} Q_{mn,t} = Q^g_{n,t} - Q^d_{n,t} \quad \forall t \in T, m \in N \tag{22}$$

$$V^{sqr}_{m,t} - V^{sqr}_{n,t} = 2 \left(R_{mn} P_{mn,t} + X_{mn} Q_{mn,t} \right)$$
$$- \frac{Z^2_{mn}}{\tilde{V}^2_{n,t}} \left(\tilde{P}_{mn,t} P_{mn,t} + \tilde{Q}_{mn,t} Q_{mn,t} \right) \quad \forall t \in T, mn \in L \tag{23}$$

$$V^{sqr}_{m,t} \bar{I}^2_{mn} \geq \sum_{\lambda}^{\Lambda} \rho_{mn,\lambda} \left(\Delta^P_{mn,t,\lambda} + \Delta^Q_{mn,t,\lambda} \right)$$
$$\forall t \in T, mn \in L \tag{24}$$

$$P_{mn,t} = P^+_{mn,t} - P^-_{mn,t} \qquad \forall t \in T, mn \in L \tag{25}$$

$$Q_{mn,t} = Q^+_{mn,t} - Q^-_{mn,t} \qquad \forall t \in T, mn \in L \tag{26}$$

$$P^+_{mn,t} + P^-_{mn,t} = \sum_{\lambda}^{\Lambda} \Delta^P_{mn,t,\lambda} \qquad \forall t \in T, mn \in L \tag{27}$$

$$Q^+_{mn,t} + Q^-_{mn,t} = \sum_{\lambda}^{\Lambda} \Delta^Q_{mn,t,\lambda} \qquad \forall t \in T, mn \in L \tag{28}$$

$$P^+_{mn,t}, P^-_{mn,t}, Q^+_{mn,t}, Q^-_{mn,t} \geq 0 \qquad \forall t \in T, mn \in L \tag{29}$$

$$0 \leq \Delta^P_{mn,t,\lambda} \leq \overline{\Delta}_{mn} \quad \forall t \in T, mn \in L, \lambda = 1, \dots, \Lambda \tag{30}$$

$$0 \leq \Delta^Q_{mn,t,\lambda} \leq \overline{\Delta}_{mn} \quad \forall t \in T, mn \in L, \lambda = 1, \dots, \Lambda \tag{31}$$

$$\rho_{mn,\lambda} = (2\lambda - 1) \overline{\Delta}_{mn} \qquad \forall mn \in L \tag{32}$$

$$\overline{\Delta}_{mn} = \overline{V} \bar{I}_{mn} / \Lambda \qquad \forall mn \in L \tag{33}$$

The key feature of this novel QP formulation, compared to the QCP, is that it avoids the use of quadratic constraints needed to represent the power losses; in this particular case required to calculate $I^{sqr}_{mn,t}$. This could be accomplished by using actual, historic or estimated voltage and power flow values ($\tilde{V}^{sqr}_{m,t}$, $\tilde{P}_{mn,t}$ and $\tilde{Q}_{mn,t}$) to approximate the power losses, as shown in (21)-(23); nevertheless, a cold-start can also be used for these values. Since the line power losses are smaller than the power flow, these approximations introduce a relatively small error in the power balance equations (21)-(22). Similarly, the approximation made in the second term of the right-hand of (23) leads to negligible errors in the voltage drop calculation as it is related to losses and, therefore, corresponds to a much smaller value than that of the first term.

The changes made in (21)-(23), compared to (14)-(16), make it possible to replace the quadratic constraint (18) using linear expressions, leading to a QP formulation instead of a QCP one. Considering that the objective function of the QP model for the AC OPF is quadratic (with positive coefficients) and the constraints are linear equations, then the QP model is a convex formulation.

The proposed QP formulation effectively approximates the AC OPF with an objective function and power balance equations that do not explicitly depend on currents as variables but on current limits and estimated voltages which are constant. The advantage is that if there is no current violation, the auxiliary variables ($\Delta^P_{mn,t,\lambda}$ and $\Delta^Q_{mn,t,\lambda}$) could take any value within their limits, defined by (30) and (31), thus resulting in less computational effort in the solution process.

Given that future distribution networks might not be fully observable, here it is proposed a two-stage approach to estimate the voltage and power flow magnitudes used to approximate the losses. In the first stage, the QP problem (19)-(33) is solved using nominal voltages for $\tilde{V}^{sqr}_{m,t}$ (i.e., a cold start) and the sum of injected power downstream line mn for $\tilde{P}_{mn,t}$ and $\tilde{Q}_{mn,t}$ (i.e., neglecting losses). The solution of the first stage is then used to initialize the second stage. The QP problem is solved again to produce the final solution. It is important to highlight that the first stage corresponds to a solution with a good accuracy and, therefore, if computational effort is an issue, the actual implementation of the proposed approach could neglect the second stage.

III. APPLICATIONS OF THE AC OPF IN DISTRIBUTION NETWORK CONTROL PROBLEMS

The formulations for the AC OPF problem presented in Section II are modified to cater for the following problems in the control of distribution networks: (1) management of DG units to maximize renewable energy harvesting; and, (2) control of capacitors to minimize energy losses. Four tests were considered to assess scalability.

A. Management of DG Units to Maximize Energy Harvesting

In this problem, renewable DG units (e.g., a photovoltaic farm) are managed to ensure the network operates without thermal or voltage problems [11], [12]. The objective is to maximize the corresponding renewable energy harvesting, i.e., curtailment is minimized. Thus, instead of minimizing the energy losses as presented in Section II, the optimization model considers the objective function (34) in which the control variables are the power output of the DG units. The uncertainties of the renewable sources are represented through a set of scenarios S (indexed by s), each of them with a given probability π_s.

$$\max \sum_{s \in S} \sum_{t \in T} \sum_{m \in DG} \pi_s \Delta_t P^g_{m,t,s} \qquad (34)$$

The power outputs of the DG units ($P^g_{m,t,s}$) are continuous variables and satisfy the DG capability limits (9)-(11). The variables that represent the operation of the network in the formulations presented in Section II (e.g., voltages, currents, and power flows) are also adapted to include the index.

To ensure network constraints are satisfied across scenarios, a common DG power output limit, $P^{lim}_{m,t}$, needs to be identified. For some scenarios, this limit will result in curtailment (e.g., due to high generation and low demand) whilst in others this limit might be above the available renewable resource, i.e., no need of curtailment. The actual DG output for each scenario is therefore calculated as the minimum value between $P^{lim}_{m,t}$ and the power that would result from the available renewable source in that scenario, $P^{av}_{t,s}$. This is shown in (35).

$$P^g_{m,t,s} = min\left(P^{av}_{t,s}, P^{lim}_{m,t}\right) \quad \forall s \in S, t \in T, m \in DG \qquad (35)$$

Consequently, the objective function maximizes the renewable energy harvesting over these multiple scenarios considering their corresponding probabilities and a constraint that finds the power output limit per DG unit (at each time period of the studied horizon) that ensures network constraints are not violated.

B. Control of Capacitors to Minimize Energy Losses

The minimization of energy (or power) losses has been traditionally studied considering capacitor banks [2], [16]. Here, this problem is considered from the operational perspective, i.e., managing switchable capacitors to minimize energy losses and maintain voltages within statutory limits. For this purpose, the AC OPF model is modified to include the injection of reactive power related to the capacitors. The power injection of a capacitor is represented by the term $Q^c_m \pi_{m,t}$, in which Q^c_m is the size of the capacitor at node m and $\pi_{m,t}$ is a binary variable related to the connection state (1 "on" and 0 "off") of the capacitor located at node m in time period t. Thus, the control actions for this problem are discrete. This new term is added to the right-hand side of (4), (15), and (22).

The incorporation of discrete variables transforms the AC OPF model into a Mixed-Integer Programming (MIP) formulation, which is harder to solve than those involving
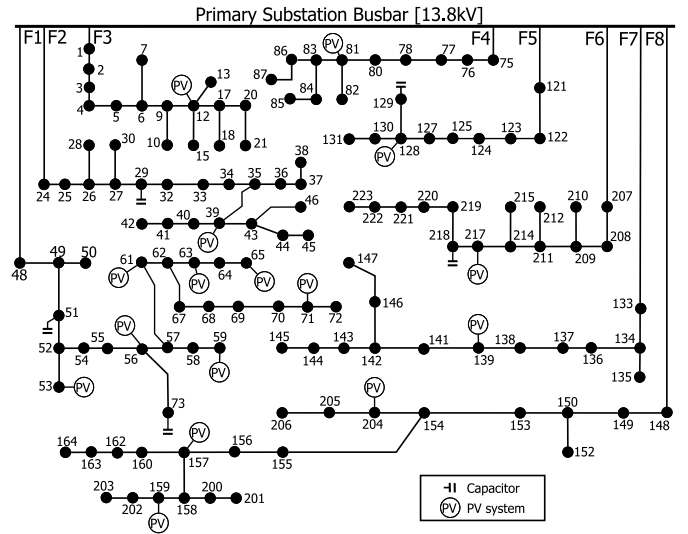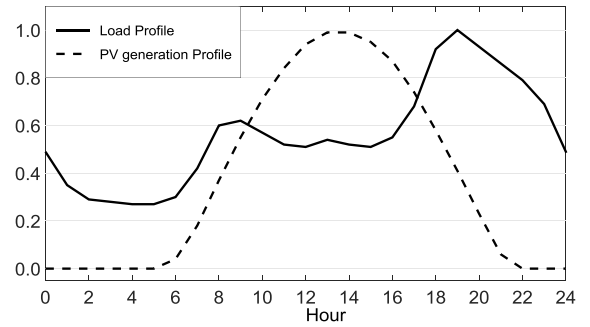

Fig. 3. Topology of the 136-node network.

Fig. 4. Normalized load and available PV generation profiles.

only continuous variables. Thus, this problem can test the performance of the formulations presented in Section II.

IV. CASE STUDY

The AC OPF formulations described in Section II are tested using a real 136-node Brazilian distribution network presented in [36]. The busbar of the primary substation has a nominal voltage of 13.8 kV and supplies 8 feeders that are operated radially. The current limit in all the lines is 180 A and the peak load is 18.3 MW and 7.9 Mvar. Voltage limits $\underline{V}$ and $\overline{V}$ are considered to be 0.90 pu and 1.10 pu. The topology of the network is illustrated in Fig. 3. The time-varying nature of the (mainly residential) loads is modelled using the normalized daily profile shown in Fig. 4, which considers 24 time periods. It also includes a maximum photovoltaic generation profile (resulting from ideal irradiance) used in Section IV-A.

The mathematical models for the two problems presented in Section III were written in the modeling language AIMMS [37]. The Two-Stage Procedure, described in Section II, was applied in the solution of the QP formulation and results are shown for both stages. The well-known solver CPLEX was used to solve the QP, QCP, MIQP, and MIQCP problems. The convex optimization solver MOSEK (within the MATLAB environment) was also used to solve the QCP and MIQCP problems; however, no improvement was

found in comparison with CPLEX. The convex formulations are compared against the more complex NLP problems using two different solvers (IPOPT and CONOPT) to increase the chances of the best solution possible. Additionally, the linear approaches for the AC OPF presented in [38] (a cold-start linear model derived from the existence of a practical solution of the nonlinear power flow equations) and [39] (based on a polyhedral relaxation of the cosine function in the power flow equations) were used to compare the performance of the proposed formulation.

The mathematical models were solved in a computer with an Intel i7-4770 processor. Eight discretization intervals (Λ) were used.

A. Management of DG Units to Maximize Renewable Energy Harvesting

The QP, QCP, and NLP formulations are adapted as described in Section III-A to solve the DG management problem considering the 136-node distribution network. For this purpose, 16 medium-scale photovoltaic (PV) systems are placed among the 8 feeders, each with a capacity of 1MW and operating at unity power factor. Specifically, the PV systems are connected to nodes 13, 39, 53, 56, 59, 61, 63, 65, 71, 81, 128, 139, 157, 159, 204, and 217 (as shown in Fig. 3). More PV capacity is allocated to Feeder 1 in order to stress the utilization of the lines.

1) Single Scenario Comparison: First, the performance of the formulations are compared in a simple fashion considering a single scenario. For this purpose, the PV generation profile in Fig. 4 is used (maximum PV generation resulting from ideal irradiance). Four tests are carried out considering single and multiple time periods. For the first test, the time period 14 (i.e., 2 pm) is considered as it corresponds to the highest PV generation. Without the optimal management of the PV systems, thermal problems occur in the network, particularly in Feeder 1 (the capacity of line 51-52 is exceeded by 28.6%). In the second test, besides 2 pm, time periods 5 and 19 (corresponding to the hours of minimum, 5 am, and maximum loading, 7 pm) are also analyzed. For the third and fourth test, 12 (from 10 am to 9 pm) and 24 (whole day) time periods are considered aiming to evaluate the scalability of the formulations (i.e., their performance when the size of the problem is increased). The current through line 51-52 and the corresponding curtailed power are shown in Fig. 5 for the fourth test.

The values of the objective function, i.e., the total harvested PV generation, for each of the four tests are shown in Table I. Both NLP solvers, IPOPT and CONOPT, obtained the same solution, although the former required less time. The solver MOSEK found the same solution as CPLEX for the QCP problem, although requiring more time. It can also be noted that due to its relaxations, the solutions of the QCP formulation are upper bounds of the optimal one (more than 1% difference in all four tests). On the other hand, due to the adopted approximations (linearizations), the solutions of the QP formulation can lead to positive or negative errors. From the mathematical perspective, the formulations result in feasible solutions.
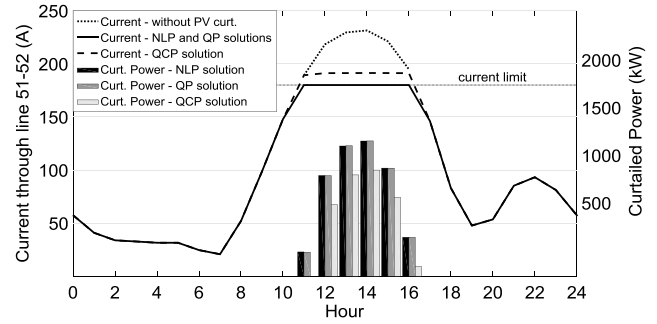

Fig. 5. Current through line 51-52 and curtailed power for the solutions of the DG management problem.

TABLE I
HARVESTED PV GENERATION (MWh) OBJECTIVE FUNCTION
OF THE DG MANAGEMENT PROBLEM

Test	Test (time periods)			
	1 (14)	2 (5,14,19)	3 (10-21)	4 (1-24)
w/o PV Management	15.84	22.40	132.96	151.20
NLP (Ipopt)	14.57	21.13	127.90	146.14
NLP (Conopt)	14.57	21.13	127.90	146.14
QCP (difference*)	14.84[**] (+1.85%)	21.40[**] (+1.28%)	129.50[**] (+1.25%)	147.74[**] (+1.09%)
QP (difference*)	14.56 (-0.07%)	21.12 (-0.05%)	127.90 (0.00%)	146.14 (0.00%)
QP - 1st stage (difference*)	14.56 (-0.08%)	21.11 (-0.06%)	127.88 (-0.02%)	146.12 (-0.02%)
Method in [38]	14.51 (-0.41%)	21.07 (-0.28%)	127.60 (-0.23%)	145.84 (-0.21%)
Method in [39]	15.84** (+8.72%)	22.40** (+6.01%)	132.96** (+3.96%)	151.20** (+3.46%)

[*] With respect to NLP Ipopt   [**] Technically infeasible solution

However, due to the relaxations used by the QCP formulation, the resulting control variables are not technically feasible (as verified using a conventional power flow) given that do not satisfy the equality in (18), thus resulting in PV injections that lead to thermal problems in Feeder 1. Indeed, the harvested energy from the QCP formulation is larger than the one from the NLP solution (Table I).

It is important to highlight that in the investigated tests, the QCP formulation leads to technically infeasible solutions. This is because its relaxation allows the current in some lines, and hence the power losses, to be larger than that using an exact formulation. This means that the QCP formulation might consider possible to have more DG injections (and corresponding reverse power flows) than what some of the lines can actually handle. This issue does not affect the QP formulation because the current limits are decoupled from the other constraints. An equivalent objective function for the QCP formulation could be used to obtain a feasible solution; that function might consider the minimization of the injected power at the substation, which implicitly minimizes the energy losses thus satisfying the condition for the QCP to be exact.

On the other hand, the QP formulation reaches a very close agreement with the values found by the NLP (the benchmark) whilst also avoiding thermal problems by effectively reducing the output of PV systems. For instance, as shown in Fig. 5,

TABLE II
PROCESSING TIME (S) - DG MANAGEMENT PROBLEM

Test	NLP (Ipopt)	NLP (Conopt)	QCP (CPLEX)	QP	QP 1st stage	Method in [38]	Method in [39]
1	0.1	0.1	0.1	0.01	0.01	0.01	0.1
2	0.3	0.3	0.1	0.02	0.01	0.05	0.3
3	1.9	5.7	0.6	0.3	0.2	0.2	0.5
4	3.8	26.6	1.6	0.9	0.7	0.6	1.4

Fig. 6.   PV generation profile for each scenario.

Fig. 7.   Total hourly PV generation in Feeder 1 for each scenario.

in order to keep current through line 51-52 within its limit, the total curtailed energy in the NLP and QP solutions are almost the same, although the curtailment applied to individual PV systems is different in each solution.

The solution found by the first stage of the QP formulation has a harvested energy value very close to that found by the optimal solution (difference of 0.02% caused by the error in the calculation of the current). This indicates that a simple initialization such as the cold start is good enough for the QP formulation. On the other hand, the alternative linear approaches, [38] and [39], result in solutions with larger differences caused by the corresponding approximations. For instance, disregarding the effect of the voltage in the active power flow, as assumed by [39], leads to an infeasible solution (difference of up to 8.72%).

In this case, it can be concluded that the AC OPF can be solved using either the NLP or the QP formulations. More importantly, the solutions found with the QP formulation, which have negligible errors (smaller than 0.1%) in comparison to the solutions found with the NLP, were achieved in a fraction of the time (see Table II). Furthermore, the first stage of the QP formulation provides very good quality solutions with a smaller time.

The errors in the calculation of the state variables due to the approximations made by the QP formulation were also found to be negligible. A comparison of the calculated voltages with those obtained using a conventional AC power flow shows maximum errors of 0.000225 pu and 0.000037 pu for the first stage and the two-stage QP, corresponding to node 71 at 1 pm (actual value of 1.019974 pu). An additional test carried out in a larger Brazilian distribution network (1,000+ nodes) showed that the error in the calculation of voltages remain small given that losses will still be just a fraction of the power flows and voltages will be kept close to nominal values (e.g., $\pm10\%$).

2) QP Formulation With Multiple Scenarios: The proposed QP formulation was applied considering 24 time periods and four different scenarios for the PV generation, each of them with the same probability ($\pi_s = 0.25$). The first scenario, shown in Fig. 6, has the same PV profile used in the previous tests (maximum PV generation), while the remaining scenarios represent high, medium, and low PV generation (produced using the tool in [40]). Considering these four scenarios, the expected harvested PV generation without PV management is 89.52 MWh (less than the 151.2 MWh with only scenario 1, Table I).

To avoid thermal problems in Feeder 1, as discussed in Section IV-A1, the proposed QP formulation defines the most suitable power output limits ($P_{m,t}^{lim}$) for the PV systems so as
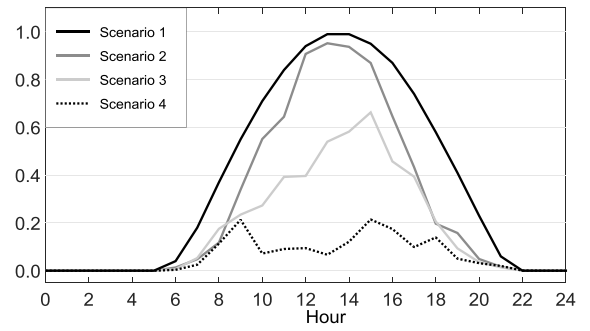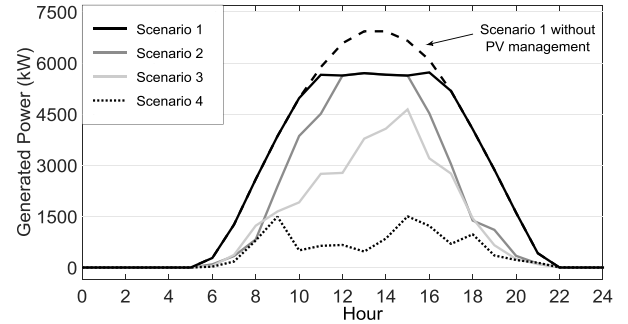
to maximize energy harvesting across scenarios. This resulted in an expected harvested PV generation of 87.5 MWh, i.e., a curtailment of only 2.3%. The corresponding total hourly PV generation in Feeder 1 is illustrated in Fig. 7 for each scenario. It can be observed that the defined limits lead to PV curtailment in scenarios 1 and 2 in which the available renewable resource is high. Moreover, no curtailment is needed in scenarios 3 and 4 as the renewable resource is low and does not create network issues.

From the computational perspective, the time required to process multiple scenarios, as expected, increases. The investigated four scenarios required 4.3 s, i.e., 4.8 times that of only one scenario (see Table I, Test 4). Although the computational time is increased, by catering for multiple scenarios the QP formulation is able to find the most suitable settings across them whilst ensuring network constraints are not violated. Therefore, in the context of renewables and future loads, similar formulations are likely to bring advantages over deterministic approaches that are limited to a single scenario (using average or worst-case values).

B. Control of Capacitors to Minimize Energy Losses

The minimization of energy losses is now solved for the 136-node network considering five 600 kvar switchable capacitors located at nodes 29, 51, 73, 129, and 218. Four tests are carried out with the MIP formulations presented in Section III-B using the same time periods considered in the previous case. The stopping criteria for the solution of the MIP models were a time limit of 1,000 s and a relative gap (relative difference between the best integer solution and the best relaxed one) of 0.01%. This small value is chosen to allow the solver to perform a thorough search without significantly

TABLE III
ENERGY LOSSES (kWh)-OBJECTIVE FUNCTION
OF THE CAPACITOR CONTROL PROBLEM

Test		1	2	3	4
MINLP AOA+Ipopt		80.80	410.27	1770.52	2623.14
MINLP AOA+Conopt		80.80 (+0.00%)	410.27 (+0.00%)	1771.03 (+0.03%)	2623.28 (+0.01%)
MIQCP - CPLEX (difference*)		79.71 (-1.35%)	405.45 (-1.17%)	1763.63 (-0.39%)	2592.44 (-1.17%)
MIQP (difference*)	OF	79.64 (-1.44%)	404.55 (-1.39%)	1760.78 (-0.55%)	2588.21 (-1.33%)
	AEL	79.71 (-1.35%)	405.45 (-1.17%)	1763.63 (-0.39%)	2591.99 (-1.19%)
MIQP 1st stage (difference*)	OF	77.94 (-3.54%)	389.43 (-5.08%)	1702.14 (-3.86%)	2509.52 (-4.33%)
	AEL	79.71 (-1.35%)	405.45 (-1.17%)	1763.63 (-0.39%)	2591.99 (-1.19%)
Method in [38]	OF	79.00 (-2.23%)	387.34 (-5.59%)	1694.43 (-4.30%)	2514.67 (-4.14%)
	AEL	79.74 (-1.31%)	405.52 (-1.16%)	1765.98 (-0.26%)	2597.51 (-0.98%)
Method in [39]	OF	44.44 (-45.00%)	280.0 (-31.75%)	1170.79 (-33.87%)	1637.85 (-37.56%)
	AEL	83.41 (+3.23%)	421.05 (+2.63%)	1836.24 (+3.71%)	2704.25 (+3.09%)

* With respect to MINLP AOA+Ipopt

TABLE IV
PROCESSING TIME (S) - CAPACITOR CONTROL PROBLEM

Test	MINLP AOA +Ipopt	MINLP AOA +Conopt	MIQCP (CPLEX)	MIQP	MIQP 1st stage	Method in [38]	Method in [39]
1	5.2	9.0	5.2	0.3	0.3	0.4	0.3
2	11.8	28.4	11.8	0.7	0.7	0.5	1.0
3	71.2	97.9	71.2	7.6	6.8	1.6	4.7
4	263.5	273.5	1000.0	11.5	10.5	3.5	9.1

TABLE V
HOURLY CONNECTION STATE OF THE CAPACITORS
IN THE MIQP SOLUTION (✓ IS "ON")

Bus	Hour																							
	1	2	3	4	5	6	7	8	9	10	11	12	13	14	15	16	17	18	19	20	21	22	23	24
29	✓	✓	✓			✓	✓	✓	✓	✓	✓	✓	✓	✓	✓	✓	✓	✓	✓	✓	✓	✓	✓	✓
51	✓	✓	✓			✓	✓										✓	✓	✓	✓				
73							✓	✓	✓	✓	✓	✓	✓	✓	✓	✓	✓	✓	✓	✓	✓	✓	✓	✓
129																	✓	✓	✓	✓	✓	✓	✓	
218	✓	✓	✓				✓	✓	✓	✓	✓	✓	✓	✓	✓	✓	✓	✓	✓	✓	✓	✓	✓	✓

in the first three tests. However, for the more demanding test 4 the MIQP model found a slightly better solution (both MIQCP solvers CPLEX and MOSEK reached the time limit). This suggests that the proposed MIQP model is likely to outperform the MIQCP formulation in applications where time is of critical importance.

Furthermore, as verified using a conventional power flow, the solutions found by these convex models result in slightly less losses (between 0.39% and 1.35%, larger than the relative gap) than the ones provided by the MINLP formulation; illustrating their effectiveness. Moreover, the MIQP formulation provides better solutions than the linearized models.

The formulations used all capacitors during peak hours. However, the convex models were able to provide a flexible operation of the capacitors particularly outside peak hours within which their disconnection resulted in lower losses. This, in turn, resulted in 10 and 13 capacitor switching actions for the MIQCP and the MIQP models, respectively; higher than the 2 actions required by the MINLP. Such effect can be catered for by constraining the switching actions.

In terms of computational performance, the significant advantage of the MIQP formulation is much more evident. Indeed, for the daily analysis (test four) the MIQP requires about 5% of the time required by the MINLP. On the other hand, the QCP reaches the time limit. Although, QP and QCP models can be solved using Interior Point methods, which have a polynomial time complexity (considering the mathematical worst case), the results show that the proposed QP model offers better performance in practical scenarios.

For test 4, the MIQP formulation found a better solution than the MIQCP model (within the time limit). Given that, in theory, the latter can provide at least the same solution, an additional attempt was carried out disregarding the time limit criterion. After 36 hours of the solution process (stopped due to storage limitations), a better objective function was obtained (2592.01 kWh). However, not only this value is slightly worse than the solution provided by the MIQP formulation (2591.99 kWh) but the required time makes it inadequate for real-time applications.

The errors for the voltage at node 203 (lowest voltage), considering the connection state of the capacitors in Table V, are shown for time periods 5, 14, and 19 in Table VI. These errors are calculated using as benchmark the values obtained with the MINLP model. Since no errors were found with the MIQCP formulation, the corresponding results are not shown. From Table VI, it can be seen that the error of the MIQP formulation is very small. Moreover, the first stage of the MIQP

compromising solution time. It must be noted that, in this case (minimization of losses), the solution of the MIQCP formulation is a lower bound of the optimal one. On the other hand, due to the linearizations adopted by the MIQP formulation, the corresponding solution is an approximation.

The Mixed-Integer NLP (MINLP) problem was solved using the *AIMMS Outer Approximation* (AOA) algorithm [41] (available in AIMMS), along with the NLP solvers IPOPT and CONOPT. A stopping criterion of 10 iterations (larger values did not lead to improvements).

In this case, all formulations found technically feasible solutions, i.e., there are no violations of voltage and current limits. The results for the four tests are shown in Table III and Table IV. Additionally, the hourly connection state of the capacitors in the MIQP solution is presented in Table V.

In Table III, the values in parentheses correspond to the difference with the solution for the MINLP formulation using AOA+IPOPT (the benchmark). The use of AOA+CONOPT led to slightly worse solutions for tests 3 and 4 and required more time. For the MIQP and the linearized models, besides the Objective Function (OF), the Actual Energy Losses (AEL), calculated using a conventional power flow, are also shown. The difference between the OF and AEL is caused by the approximations made in the MIQP formulation (about 0.2% for the tests in Table III). The MIQCP and the MIQP convex models found the same solution for the state of the capacitors

TABLE VI
ERROR FOR VOLTAGE CALCULATED AT NODE 203
(pu) -CAPACITOR CONTROL PROBLEM

Time Period	MINLP minimum voltage	MIQP error*	MIQP 1st stage error*	Method in [38] error*	Method in [39] error*
5	0.982478	0.000000	0.000006	0.000496	-0.007322
14	0.965519	0.000001	0.000051	0.001901	-0.013832
19	0.930652	0.000009	0.000412	0.007508	-0.025212

* With respect to MINLP

formulation presents relatively small errors when compared with the methods in [38] and [39]. These results not only demonstrate the accuracy of the proposed method but also that the second stage could indeed be neglected to further reduce the computational efforts.

V. DISCUSSION

The tests carried out for the DG Management and the Capacitor Control problems allowed the evaluation of the efficiency, robustness, and scalability of the proposed QP formulation. The results indicate that the QP formulation is efficient given that more demanding tests for either of the problems did not have a significant impact on the computational effort. The QP formulation was able to provide feasible solutions for either of the problems and, in some cases, even better solutions than the conventional formulations; thus demonstrating its robustness. Finally, the QP formulation was shown to be scalable as it was capable of finding good solutions with relatively low computational effort when the dimensions of the problems were increased.

While the first stage of the proposed QP formulation has led to good quality solutions, as shown in the results for the different cases and tests, the second stage was effective in reducing errors. Other methods based on linearization, such as [38] and [39], are likely to benefit from similar refinements.

Finally, although the proposed QP formulation is per se deterministic, it was demonstrated it can be extended to also consider multiple scenarios to cater for uncertainties related to renewable generation. Further, more complex adaptations can be carried out to incorporate, for instance, demand uncertainties and probabilistic constraints.

VI. CONCLUSION

The complex decision making processes required by Smart Grid schemes controlling network elements and participants can be solved tailoring optimization approaches such as the well-known AC Optimal Power Flow (OPF). This work proposes and demonstrates a novel Quadratic Programming (QP) formulation as an efficient, scalable and robust alternative to solve the AC OPF problem in smart distribution networks. The approach is compared against the more established Non-Linear Programming (NLP), linearized and Quadratically Constrained Programming (QCP) formulations.

The performance of the models was assessed in two cases: (1) management of distributed generation units to minimize energy losses (continuous control variables); and, (2)

control of capacitors to minimize energy losses (discrete control variables). Four tests were considered to assess scalability.

The results demonstrate that the proposed QP formulation outperforms conventional formulations for the AC OPF. In all cases and tests, the QP formulation was solved in significantly smaller computational times than the other NLP and QCP formulations. Moreover, the QP model found solutions of best or at least equal quality for the problems, which showed the scalability and robustness of the proposed approach.

The additional complexity due to the presence of discrete variables was successfully dealt with by the QP formulation in the studied cases. The QCP, although provided good solutions, required significant computational time. Furthermore, in the first case, the QCP formulation resulted in infeasible solutions, i.e., network constraints were violated.

Based on the above, it can be concluded that the QP formulation is an efficient and robust approach to solve the AC OPF problem tailored to cater for diverse network control challenges. Therefore, this formulation is a suitable alternative to be at the heart of the decision making of complex, real-time schemes to be adopted by future Smart distribution networks.

APPENDIX

EXTENSION OF THE QP FORMULATION FOR UNBALANCED NETWORKS

The QP formulation introduced in Section II-C can be extended to represent the unbalanced (three-phase) operation of distribution networks. Power losses in line mn and phase ϕ are calculated as $S^L_{mn,\phi,t} = \Delta V_{mn,\phi,t} \, I^*_{mn,\phi,t}$. They can be written in terms of the power through line mn ($S_{mn,\phi,t} = P_{mn,\phi,t} + jQ_{mn,\phi,t}$ for phase ϕ), and the impedance of line mn ($Z_{mn,\phi,\psi} = R_{mn,\phi,\psi} + jX_{mn,\phi,\psi}$, between phases ϕ and ψ), as shown in (36). Using actual, historic or estimated values for the voltage in bus m and phase ϕ ($\tilde{V}_{m,\phi,t}$), as well as for the power through line mn ($\tilde{S}_{mn,\phi,t} = \tilde{P}_{mn,\phi,t} + j\tilde{Q}_{mn,\phi,t}$), (36) can be re-written using the linear expression given by (37).

$$S^L_{mn,\phi,t} = \left[\sum_{\psi} Z_{mn,\phi,\psi}\left(\frac{S_{mn,\psi,t}}{V_{m,\psi,t}\angle\theta_\psi}\right)^*\right]\left(\frac{S_{mn,\phi,t}}{V_{m,\phi,t}\angle\theta_\phi}\right) \quad (36)$$

$$S^L_{mn,\phi,t} = \sum_{\psi} \frac{Z'_{mn,\phi,\psi}\tilde{S}^*_{mn,\phi,t}}{\tilde{V}_{m,\phi,t}\tilde{V}_{m,\psi,t}} S_{mn,\psi,t} \quad (37)$$

in which $Z'_{mn,\phi,\psi}$ is an equivalent impedance defined as $Z_{mn,\phi,\psi}\angle(\theta_\psi - \theta_\phi)$. This parameter is derived assuming that the phase angle unbalance is small, i.e., $\theta_\psi - \theta_\phi$ can be calculated using flat start values. The linear approximation for the power losses in (37) can be used to represent the active and reactive power balance, as shown in (38) and (39).

$$\sum_{km\in L}\left[P_{km,\phi,t} + \text{Re}\left\{S^L_{mn,\phi,t}\right\}\right]$$
$$- \sum_{mn\in L} P_{mn,\phi,t} = P^g_{m,\phi,t} - P^d_{m,\phi,t} \quad (38)$$

$$\sum_{km \in L} \left[Q_{km,\phi,t} + \text{Im}\left\{ S^L_{mn,\phi,t} \right\} \right]$$
$$- \sum_{mn \in L} Q_{mn,\phi,t} = Q^g_{m,\phi,t} - Q^d_{m,\phi,t} \qquad (39)$$

Furthermore, the voltage drop in line *mn* and phase ϕ is written in terms of the equivalent impedance and the power losses, as expressed in (40). Thus, the QP formulation can be extended to represent the operation of unbalanced distribution networks using (38)-(40) for the power balance and voltage drop equations, instead of (21)-(23).

$$V^{sqr}_{m,\phi,t} - V^{sqr}_{n,\phi,t} = 2 \sum_{\psi} \left(\text{Re}\{ Z'_{mn,\phi,\psi} \} P_{mn,\phi,t} \right.$$
$$\left. + \text{Im}\{ Z'_{mn,\phi,\psi} \} Q_{mn,\phi,t} \right) - \sum_{\psi} \left| Z'_{mn,\phi,\psi} S^L_{mn,\psi,t} \right|. \qquad (40)$$

REFERENCES

[1] A. Keane *et al.*, "State-of-the-art techniques and challenges ahead for distributed generation planning and optimization," *IEEE Trans. Power Syst.*, vol. 28, no. 2, pp. 1493–1502, May 2013.

[2] F. Capitanescu, I. Bilibin, and E. R. Ramos, "A comprehensive centralized approach for voltage constraints management in active distribution grid," *IEEE Trans. Power Syst.*, vol. 29, no. 2, pp. 933–942, Mar. 2014.

[3] S. Bruno, S. Lamonaca, G. Rotondo, U. Stecchi, and M. La Scala, "Unbalanced three-phase optimal power flow for smart grids," *IEEE Trans. Ind. Electron.*, vol. 58, no. 10, pp. 4504–4513, Oct. 2011.

[4] E. Dall'Anese, H. Zhu, and G. B. Giannakis, "Distributed optimal power flow for smart microgrids," *IEEE Trans. Smart Grid*, vol. 4, no. 3, pp. 1464–1475, Sep. 2013.

[5] J. Carpentier, "Contribution to the economic dispatch problem," *Bull. de la Société Française des Elect.*, vol. 3, no. 8, pp. 431–447, 1962.

[6] A. J. Wood, B. F. Wollenberg, and G. B. Sheblé, *Power Generation, Operation, and Control*. New York, NY, USA: Wiley, 2013.

[7] G. P. Harrison and A. R. Wallace, "Maximising distributed generation capacity in deregulated markets," in *Proc. IEEE PES Transm. Distrib. Conf. Expo.*, vol. 2. Dallas, TX, USA, 2003, pp. 527–530.

[8] L. F. Ochoa, C. J. Dent, and G. P. Harrison, "Distribution network capacity assessment: Variable DG and active networks," *IEEE Trans. Power Syst.*, vol. 25, no. 1, pp. 87–95, Feb. 2010.

[9] P. N. Vovos, G. P. Harrison, A. R. Wallace, and J. W. Bialek, "Optimal power flow as a tool for fault level-constrained network capacity analysis," *IEEE Trans. Power Syst.*, vol. 20, no. 2, pp. 734–741, May 2005.

[10] Y. M. Atwa, E. F. El-Saadany, M. M. A. Salama, and R. Seethapathy, "Optimal renewable resources mix for distribution system energy loss minimization," *IEEE Trans. Power Syst.*, vol. 25, no. 1, pp. 360–370, Feb. 2010.

[11] L. F. Ochoa and G. P. Harrison, "Minimizing energy losses: Optimal accommodation and smart operation of renewable distributed generation," *IEEE Trans. Power Syst.*, vol. 26, no. 1, pp. 198–205, Feb. 2011.

[12] M. J. Dolan, E. M. Davidson, I. Kockar, G. W. Ault, and S. D. J. Mcarthur, "Distribution power flow management utilizing an online optimal power flow technique," *IEEE Trans. Power Syst.*, vol. 27, no. 2, pp. 790–799, May 2012.

[13] S. W. Alnaser and L. F. Ochoa, "Advanced network management systems: A risk-based AC OPF approach," *IEEE Trans. Power Syst.*, vol. 30, no. 1, pp. 409–418, Jan. 2015.

[14] Y. Zhu and K. Tomsovic, "Optimal distribution power flow for systems with distributed energy resources," *Int. J. Elect. Power Energy Syst.*, vol. 29, no. 3, pp. 260–267, 2007.

[15] M. B. Liu, C. A. Canizares, and W. Huang, "Reactive power and voltage control in distribution systems with limited switching operations," *IEEE Trans. Power Syst.*, vol. 24, no. 2, pp. 889–899, May 2009.

[16] A. Borghetti, "Using mixed integer programming for the volt/var optimization in distribution feeders," *Elect. Power Syst. Res.*, vol. 98, pp. 39–50, May 2013.

[17] H. M. Khodr, J. Martinez-Crespo, M. A. Matos, and J. Pereira, "Distribution systems reconfiguration based on OPF using benders decomposition," *IEEE Trans. Power Del.*, vol. 24, no. 4, pp. 2166–2176, Oct. 2009.

[18] R. A. Jabr, R. Singh, and B. C. Pal, "Minimum loss network reconfiguration using mixed-integer convex programming," *IEEE Trans. Power Syst.*, vol. 27, no. 2, pp. 1106–1115, May 2012.

[19] E. Romero-Ramos, J. Riquelme-Santos, and J. Reyes, "A simpler and exact mathematical model for the computation of the minimal power losses tree," *Elect. Power Syst. Res.*, vol. 80, no. 5, pp. 562–571, 2010.

[20] H. L. Hijazi and S. Thiébaux, "Optimal AC distribution systems reconfiguration," in *Proc. Power Syst. Comput. Conf. (PSCC)*, Wrocław, Poland, 2014, pp. 1–7.

[21] R. Romero, J. F. Franco, F. B. Leão, M. J. Rider, and E. S. de Souza, "A new mathematical model for the restoration problem in balanced radial distribution systems," *IEEE Trans. Power Syst.*, vol. 31, no. 2, pp. 1259–1268, Mar. 2016.

[22] L. Gan and S. H. Low, "Convex relaxations and linear approximation for optimal power flow in multiphase radial networks," in *Proc. 18th Power Syst. Comput. Conf.*, Wrocław, Poland, 2014, pp. 1–9.

[23] K. S. Pandya and S. K. Joshi, "A survey of optimal power flow methods," *J. Appl. Inf. Technol.*, vol. 4, no. 5, pp. 450–458, 2008.

[24] R. A. Jabr, "Radial distribution load flow using conic programming," *IEEE Trans. Power Syst.*, vol. 21, no. 3, pp. 1458–1459, Aug. 2006.

[25] M. Farivar and S. H. Low, "Branch flow model: Relaxations and convexification—Part I," *IEEE Trans. Power Syst.*, vol. 28, no. 3, pp. 2554–2564, Aug. 2013.

[26] J. Lavaei, A. Rantzer, and S. Low, "Power flow optimization using positive quadratic programming," in *Proc. 18th IFAC World Congr.*, Milan, Italy, 2011, pp. 10481–10486.

[27] X. Bai, H. Wei, K. Fujisawa, and Y. Wang, "Semidefinite programming for optimal power flow problems," *Int. J. Elect. Power Energy Syst.*, vol. 30, nos. 6–7, pp. 383–392, 2008.

[28] J. F. Franco, M. J. Rider, and R. Romero, "A mixed-integer quadratically-constrained programming model for the distribution system expansion planning," *Int. J. Elect. Power Energy Syst.*, vol. 62, pp. 265–272, Nov. 2014.

[29] R. C. Burchett, H. H. Happ, and D. R. Vierath, "Quadratically convergent optimal power flow," *IEEE Trans. Power App. Syst.*, vol. PAS-103, no. 11, pp. 3267–3275, Nov. 1984.

[30] I. M. Nejdawi, K. A. Clements, and P. W. Davis, "An efficient interior point method for sequential quadratic programming based optimal power flow," *IEEE Trans. Power Syst.*, vol. 15, no. 4, pp. 1179–1183, Nov. 2000.

[31] Y. Tao and A. P. S. Meliopoulos, "Optimal power flow via quadratic power flow," in *Proc. Power Syst. Conf. Expo.*, Phoenix, AZ, USA, 2011, pp. 1–8.

[32] K. Turitsyn, P. Šulc, S. Backhaus, and M. Chertkov, "Distributed control of reactive power flow in a radial distribution circuit with high photovoltaic penetration," in *Proc. IEEE PES Gener. Meeting*, Providence, RI, USA, 2010, pp. 1–6.

[33] M. Farivar, C. R. Clarke, S. H. Low, and K. M. Chandy, "Inverter VAR control for distribution systems with renewables," in *Proc. IEEE Int. Conf. Smart Grid Commun. (SmartGridComm)*, Brussels, Belgium, 2011, pp. 457–462.

[34] R. G. Cespedes, "New method for the analysis of distribution networks," *IEEE Trans. Power Del.*, vol. 5, no. 1, pp. 391–396, Jan. 1990.

[35] S. H. Low, "Convex relaxation of optimal power flow—Part II: Exactness," *IEEE Trans. Control Syst. Technol.*, vol. 1, no. 2, pp. 177–189, Jun. 2014.

[36] J. R. S. Mantovani, F. Casari, and R. A. Romero, "Reconfiguração de sistemas de distribuição radiais utilizando o critério de queda de tensão," *Revista Brasileira de Controle Automação SBA*, vol. 11, no. 3, pp. 150–159, 2000.

[37] J. Bisschop and M. Roelofs, *AIMMS—The User's Guide*. Paragon Decis. Technol., Haarlem, The Netherlands, 2006.

[38] S. Bolognani and S. Zampieri, "On the existence and linear approximation of the power flow solution in power distribution networks," *IEEE Trans. Power Syst.*, vol. 31, no. 1, pp. 163–172, Jan. 2016.

[39] C. Coffrin and P. Van Hentenryck, "A linear-programming approximation of AC power flows," *INFORMS J. Comput.*, vol. 26, no. 4, pp. 718–734, May 2014.

[40] I. Richardson and M. Thomson, *Integrated Domestic Electricity Demand and PV Micro-Generation Model*, Loughborough Univ. Inst. Repository, Leicester, U.K., 2011. [Online]. Available: https://dspace.lboro.ac.uk/dspace-jspui/handle/2134/7773

[41] M. Hunting. (2011). *The AIMMS Outer Approximation Algorithm for MINLP*. [Online]. Available: http://www.aimms.com/aimms/download/white-papers/gmp-aoa-aimms-whitepaper-2011.pdf

John F. Franco (S'11–M'13) received the B.Sc. and M.Sc. degrees in electrical engineering from the Universidad Tecnológica de Pereira, Colombia, in 2004 and 2006, respectively, and the Ph.D. degree in electrical engineering from the São Paulo State University, Ilha Solteira, Brazil, in 2012.

He is currently a Professor with the São Paulo State University, Rosana, Brazil. His current research interests include the development of methodologies for the optimization and planning and control of electrical power systems.
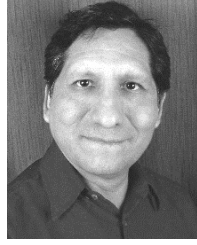
Rubén Romero (M'93–SM'08) received the B.Sc. and P.E. degrees in electrical engineering from the National University of Engineering, Lima, Perú, in 1978 and 1984, respectively, and the M.Sc. and Ph.D. degrees in electrical engineering from the University of Campinas, Brazil, in 1990 and 1993, respectively.

He is currently a Professor with the Electrical Engineering Department, São Paulo State University, Ilha Solteira, Brazil. His current research interests include electrical power systems planning.

Luis F. Ochoa (S'01–M'07–SM'12) received the B.Eng. degree from UNI, Lima, Peru, in 2000, and the M.Sc. and Ph.D. degrees from UNESP, Ilha Solteira, Brazil, in 2003 and 2006, respectively. He is a Professor of Smart Grids and Power Systems with the University of Melbourne, Australia and a Part-Time Professor of Smart Grids with the University of Manchester, U.K. His research interests include network integration and control of distributed energy resources and future low-carbon distribution networks.